

RESEARCH ARTICLE OPEN ACCESS

Optimizing Electric Vehicle Charging Infrastructure on Highways: A MILP Model for Balanced Demand Allocation

Raka Jovanovic¹  | Sertac Bayhan¹  | I. Safak Bayram² 

¹Qatar Environment and Energy Research Institute, Hamad Bin Khalifa University, Doha, Qatar | ²Department of Electronic and Electrical Engineering, University of Strathclyde, Glasgow, UK

Correspondence: I. Safak Bayram (safak.bayram@strath.ac.uk)

Received: 11 November 2025 | **Revised:** 11 January 2026 | **Accepted:** 27 January 2026

Academic Editor: Abdallah Bouabidi

Keywords: demand allocation | electric vehicles | linear programming | location and capacity optimization

ABSTRACT

The strategic placement and sizing of electric vehicle (EV) charging stations on highways are critical for alleviating range anxiety and fostering widespread EV adoption. This paper presents a novel mixed-integer linear programming (MILP) model for optimizing the location and capacity of charging stations along highway corridors. Unlike traditional approaches, our formulation explicitly models the distribution of charging demand from each origin–destination (O/D) pair among the multiple stations along its path. The nonlinearities inherent in this flow-sharing mechanism are efficiently handled via a piecewise linear approximation, ensuring model tractability for real-world instances. Using real geographical and demographic data, we generate realistic case studies for two U.S. highways, I–70 and I–95. Our analysis evaluates the trade-offs between cost, service quality, and infrastructure layout for different charger power levels (50, 150, and 350 kW) and EV adoption scenarios. Results indicate that 350 kW chargers generally offer the most cost-effective solution while significantly reducing expected user times by up to 70% compared to 50 kW chargers. The model provides a practical decision-support tool for planners, balancing computational efficiency with a high-fidelity representation of network-wide charging dynamics.

1 | Introduction

A global motivation to decarbonize the transportation sector has intensified efforts to address pressing environmental challenges exacerbated by the use of fossil fuel vehicles. The electrification of transportation, primarily through the adoption of electric vehicles (EVs), is increasingly regarded as an ideal solution. This transition is creating a pressing need for careful charging infrastructure planning. In 2023 alone, global EV registrations reached nearly 14 million, expanding the total fleet to 40 million. This represents a six-fold increase from 2018, with EVs capturing 18% of the new car market, up from just 2% 5 years prior [1]. This influx is propelled by ambitious government policies which aim to fully decarbonize road transportation; European Union and

the United Kingdom targets to phase out internal combustion engines by 2050 [2]. However, the success of this large-scale shift relies on addressing significant barriers, most notably high upfront vehicle costs and persistent consumer range anxiety [2].

This anxiety is directly linked to the challenge of public charging infrastructure. While the global network of public chargers has exceeded 5 million in 2024 [3] and the US increased its charging stock by 20% in 2024 to just under 200,000 public charging points, a large body of literature suggests its distribution is often misaligned with user demand and geographic needs. This challenge is particularly important for long-distance, inter-regional travel, which relies exclusively on high power DC charging stations. While AC charging stations (e.g., Level 1 and Level 2) can service

This is an open access article under the terms of the [Creative Commons Attribution](https://creativecommons.org/licenses/by/4.0/) License, which permits use, distribution and reproduction in any medium, provided the original work is properly cited.

Copyright © 2026 Raka Jovanovic et al. *International Journal of Energy Research* published by John Wiley & Sons Ltd.

daily commuting needs, DC charging infrastructure is the sole enabler for extended trips.

Furthermore, the operational efficiency of the DC networks is not merely a matter of quantity, but of strategy. Optimal long-distance travel, as demonstrated in recent studies, involves a counter-intuitive “hop-on, hop-off” model. This consists of more frequent, shorter charging stops to avoid low-power constant voltage charging phase which is typically beyond 80% state of charge (SoC) [4]. This model minimizes waiting times and charger utilization, but requires better coverage of charging networks [5].

To address the range anxiety and support efficient travel, massive public investment is underway. However, the high capital cost presents a critical engineering problem: what is the optimal number and placement of stations? The suitability of a location is a complex optimization problem, requiring a balance between technical needs (grid capacity), user-centered needs (safety, amenities), and geographic attributes (proximity to highways and Points of Interest) [1, 2]. Therefore, this research develops and applies a methodology to ensure maximum completion of long-distance U.S. car trips via the thoughtful placement of DCFC stations. The model is deployed to optimally locate stations across the continental U.S. highway network, providing a cost-effective roadmap to help households more rapidly adopt BEVs and accelerate the transition to a more environmentally sustainable travel mode.

The challenge of planning EV charging infrastructure has been approached from numerous angles, resulting in a rich body of literature that employs a variety of modeling paradigms and optimization techniques. These studies can be effectively classified according to their primary geographical context, methodological foundations, and specific operational considerations.

A significant portion of existing research concentrates on urban and metropolitan charging networks. Within this domain, mixed-integer linear programming (MILP) has been widely applied to determine optimal station placement and sizing, often integrating real-world datasets on population distribution and grid capacity [6]. Complementary approaches have leveraged spatial-temporal analyses of empirical travel data [7], system dynamics for campus-scale planning [8], and hybrid metaheuristics such as genetic algorithms combined with particle swarm optimization [9]. Further sophistication has been introduced through multi-criteria decision-making frameworks that incorporate fuzzy analytic hierarchy processes [10] and comprehensive socioeconomic cost models [11]. A common characteristic of these urban studies is their focus on localized travel patterns and decentralized charging demand, which differs substantially from the linear, long-distance travel patterns characteristic of highway systems.

The distinct challenges of highway corridor infrastructure have motivated a separate line of inquiry. The linear geometry of highways and the critical need to mitigate range anxiety necessitate specialized planning models. Research in this area includes multi-criteria decision support systems that weigh factors like traffic volume and proximity to interchanges [12], multi-agent simulation platforms that emulate driver charging behavior [13], and agent-based models aimed at minimizing total journey time [14]. Other contributions have proposed methodologies for estimating the required number of stations across extensive road networks [15] and hierarchical frameworks that coordinate fixed charging stations with mobile energy storage units [16]. While

these studies acknowledge the highway context, they frequently employ simplified assumptions regarding how travelers distribute their charging stops among the available facilities along a route, overlooking the interdependent nature of demand across different origin–destination (O/D) pairs.

A third prominent research pillar investigates service quality and operational performance at charging stations. Queuing theory forms the backbone of this work, with models incorporating practical constraints like finite queue lengths to prevent unrealistic assumptions [17]. Some studies integrate demand forecasting neural networks with heuristic algorithms to optimize station design under service level constraints [18], while others apply loss-queue models (M/M/c/c) in conjunction with greedy algorithms for capacity allocation [19]. Hierarchical models have also been developed that nest queuing analysis within a broader system optimization framework [20]. Although these works rightly emphasize user experience, they often rely on predetermined or simplified demand allocation schemes, which can limit the accuracy of station-level utilization estimates.

More recent investigations have expanded the scope to include power grid integration and advanced energy management. This evolving subfield encompasses the optimization of charging station power supply with vehicle-to-everything (V2X) functionality [21], strategic placement within electrical distribution networks to improve voltage profiles and reduce losses [22], and two-stage frameworks that decouple long-term design from short-term operational control [23]. Bi-level optimization techniques have been employed to model the strategic interplay between infrastructure providers and EV users [24], and several review articles offer valuable syntheses of the field’s evolution and future trajectories [25, 26].

Despite these substantial contributions, a notable gap remains in the explicit modeling of the demand distribution process across multiple charging stations serving the same travel path. The mechanism by which the total charging demand of an O/D pair is proportionally split among the active stations on its route introduces a nonlinearity that is often circumvented for computational convenience. While certain studies [27] tackle joint placement and assignment, they frequently depend on submodular function heuristics rather than a direct, path-based representation of demand splitting.

This work seeks to address these limitations by introducing a MILP model tailored for highway corridors that explicitly formulates the flow distribution mechanism. In contrast to prior approaches that simplify demand allocation [12, 13, 15], our methodology employs a piecewise linear approximation to accurately capture the reciprocal relationship governing flow sharing, thereby preserving model linearity and tractability. This allows for a more comprehensive representation of station utilization and enables the derivation of robust infrastructure plans that maintain service levels across the network. The proposed formulation successfully navigates the trade-off between model fidelity and computational performance, facilitating the solution of large-scale, realistic problem instances that have challenged previous nonlinear or oversimplified models [17–19].

This paper is structured as follows. Section 2 presents the mathematical model, including the MILP formulation and piecewise linear approximation. Section 3 details the methodology for

generating problem instances from real-world data. Section 4 analyzes two U.S. highway corridors, evaluating charger power and adoption impacts. Finally, Section 5 summarizes key findings and future research directions.

2 | Mathematical Model

This section presents the mathematical programming model developed for optimizing the locations and capacities of EV charging stations. The formulation builds upon the standard O/D pair framework commonly used to model traffic flows. In traditional formulations, the objective is typically to determine a subset of candidate charging stations and their capacities such that all O/D pairs are adequately covered by at least one station while minimizing total investment cost.

In the proposed model, this basic structure is extended to explicitly analyze how charging demand from each O/D pair is distributed among the charging stations located along its path. This extension allows a more realistic estimation of utilization and service levels across the network. Such detailed modeling is often avoided due to the nonlinear relationships that arise when distributing flow among multiple stations. However, in the proposed formulation, this issue is efficiently addressed using a linear piecewise approximation, which preserves model tractability. As a result, the model can be solved for real-world-sized instances using standard MILP solvers within reasonable computational limits.

The proposed piecewise linear framework offers a structured, tractable foundation for planning, though it simplifies real-world driver behavior influenced by waiting times, amenities, and pricing. As a result, the assumption of proportional demand allocation may underestimate uneven utilization or congestion patterns if drivers exhibit systematic station preferences.

2.1 | Model Outline

The model is based on several simplifying assumptions intended to capture the essential characteristics of the EV charging station location problem while keeping the formulation computationally manageable. It is assumed that there exists a set O of O/D pairs, where each pair $(o, d) \in O$ represents a typical route traveled by EVs between two locations, such as cities or highway exits. Each O/D pair is associated with a traffic flow λ_{od} , representing the average number of EVs per hour that traverse the route. These values can be derived from empirical mobility data or transport simulations.

A set C of potential charging station locations is considered, where each candidate site $c \in C$ can host a limited number of chargers. The parameter M_c denotes the maximum number of chargers that can be installed at location c , reflecting physical or grid-related constraints. For each O/D pair (o, d) , a subset $\text{Path}_{od} \subseteq C$ identifies the candidate charging stations that are accessible along its route.

It is further assumed that all charging stations use the same type of charger with uniform technical characteristics. Each charger has a fixed installation cost and a constant service rate μ , which represents the number of vehicles that can be fully charged per hour. The service rate μ can be derived from the charger's

nominal power and the average energy demand per session, thereby linking physical charging characteristics with the model parameters. This uniformity assumption simplifies the analysis while maintaining practical interpretability.

Regarding user behavior, it is assumed that EV charging sessions associated with each O/D pair are evenly distributed among all active stations located along its path. In other words, if multiple charging stations are installed along a route, the demand from that O/D pair is shared proportionally among them. Although simplified, this assumption provides a reasonable first-order approximation of demand allocation and enables the model to be linearized and computationally efficient.

Similarly, the model employs average, time-invariant estimates for hourly EV demand and per-session energy consumption. This focuses the analysis on long-term strategic planning rather than short-term operational variability. While this approach does not capture temporal fluctuations (e.g., peak travel periods) or heterogeneity in vehicle efficiency, it maintains tractability and ensures that the optimization reflects typical system conditions. Both simplifications allow the model to produce implementable infrastructure plans, with the understanding that more granular, data-driven parameterization can be incorporated in future adaptations.

An additional assumption of the model is the requirement to prevent extensive dead zones—segments of the highway where EV charging is not possible. To ensure adequate coverage, the set of candidate charging locations is partitioned into predefined zones, and at least one charging station must be established within each zone.

The objective of the problem is to determine which charging stations to open and how many chargers to install at each selected location, while minimizing total installation costs. Each O/D pair must be covered by at least one active charging station along its path, ensuring that every route provides feasible charging opportunities. In addition, each charging station must satisfy a service-level constraint that ensures adequate performance and user experience. Specifically, the total arrival rate of vehicles at a station must not exceed a specified fraction of its service capacity, represented by μ times the number of installed chargers. This requirement ensures that the utilization level at each station remains below a defined threshold, thereby limiting expected waiting times and ensuring operational stability.

Overall, the proposed formulation balances modeling realism and computational efficiency. By capturing demand distribution, capacity constraints, and service-level requirements within a linear approximation framework, it provides a foundation for large-scale optimization of EV charging infrastructure using standard mathematical programming tools. The detailed MILP formulation is presented in the following subsection.

2.2 | Mathematical Model With Piecewise Linear Approximation

This section presents the mathematical programming model for optimizing the location and capacity of EV charging stations based on the description given in the previous subsection. For clarity, the presentation of the model is divided into two parts. The first part describes the basic formulation, while the second

focuses on the flow-sharing constraints and the piecewise linear approximation of the reciprocal function.

2.2.1 | Basic Formulation

The base part of the model uses the following set of parameters:

- C —set of potential charging station locations, indexed by c .
- O —set of O/D pairs, indexed by (o, d) .
- Z —set of zones, index by z .
- $\text{zone}_z \subseteq C$ —subset of stations located in zone z .
- $\text{Path}_{od} \subseteq C$ —subset of stations located along the path of O/D.
- λ_{od} —hourly charging demand for O/D pair (o, d) .
- M_c —maximum number of chargers that can be installed at station c .
- μ —service rate of a single charger (vehicles charged per hour).
- τ —Quality of Service (QoS) related coefficient.
- Cost—installation cost per charger.

In addition the following set of decision variables are used:

- $x_c \in \mathbb{Z}_{\geq 0}$ —number of chargers installed at station c , which can be zero if the station is not selected (active).
- $u_c \in \{0, 1\}$ —binary variable equal to 1 if station c is active.
- $\lambda_{c,od} \geq 0$ —portion of demand λ_{od} served at station c .
- $\Lambda_c \geq 0$ —total demand (incoming flow) to station c .
- $n_{od} \geq 0$ —total number of charging stations on O/D pair (o, d) .

The objective function minimizes the total cost of installed chargers, as given by

$$\min \sum_{c \in C} \text{cost} \cdot x_c. \quad (1)$$

Equation (1) states that the goal is to minimize the sum of costs associated with each station, where the cost at each station is calculated as the product of the number of chargers x_c installed at that station and the cost per charger.

To fully specify the model, the constraints related to the decision variables and parameters must be defined. These constraints can be grouped as follows: station activation (2) and (3), zone coverage (5), coverage and flow conservation (5) and (6), station load and capacity (7) and (8) and flow-sharing with associated linearization. For clarity, the flow-sharing and linearization constraints are presented in the following subsection.

$$x_c - M_c u_c \leq 0, \quad \forall c \in C, \quad (2)$$

$$x_c - u_c \geq 0, \quad \forall c \in C, \quad (3)$$

$$\sum_{c \in \text{zone}_z} u_c \geq 1, \quad \forall z \in Z, \quad (4)$$

$$\sum_{c \in \text{Path}_{od}} u_c \geq 1, \quad \forall (o, d) \in O, \quad (5)$$

$$\sum_{c \in \text{Path}_{od}} \lambda_{c,od} = \lambda_{od}, \quad \forall (o, d) \in O, \quad (6)$$

$$\Lambda_c = \sum_{(o,d) \in O} \lambda_{c,od}, \quad \forall c \in C, \quad (7)$$

$$\Lambda_c \leq \tau \mu x_c \quad \forall c \in C, \quad (8)$$

$$x_c \in \mathbb{Z}_{\geq 0}, \quad \forall c \in C, \quad (9)$$

$$u_c \in \{0, 1\} \quad \forall c \in C, \quad (10)$$

$$\lambda_{c,od} \geq 0, \quad \forall c \in C, \forall (o, d) \in O, \quad (11)$$

$$\Lambda_c \geq 0 \quad \forall c \in C. \quad (12)$$

Constraints (2) and (3) link the binary activation variables u_c with the installed capacity x_c . Specifically, (2) ensures that chargers cannot be installed unless the station is active (corresponding to location selection), while (3) guarantees that each active station has at least one installed charger. Constraint given in (4) guarantees that there is at least one active station in each zone $z \in Z$. Equation (5) ensures that each O/D path contains at least one active station, while (6) enforces that the total demand λ_{od} of each O/D pair is fully distributed among the stations along its path. Finally, constraints (7) and (8) guarantee that the total flow arriving at each station must not exceed its service capacity. Equation (7) aggregates the flow from all O/D pairs arriving at each station, and (8) limits the total served demand according to the station's installed capacity, ensuring that the service rate μ per charger is not exceeded the expected QoS τ . Equations (9) and (10) ensure that the number of chargers x_c is a non-negative integer and the activation variables u_c are binary. Equations (11) and (12) guarantee that all assigned flows and total arrival rates are non-negative.

2.2.2 | Flow-Sharing and Linearization Constraints

To model how charging demand ($\lambda_{c,od}$) is distributed among multiple stations along each O/D path, the model introduces flow-sharing constraints. The demand share depends on the number of active stations on the path, making the formulation nonlinear. To maintain linearity and solver efficiency, a piecewise linear approximation of the reciprocal function is used.

The linearization introduces a new set of parameters b_k —breakpoints defining the piecewise linear segments for n_{od} , where $b_k \in \{1, 2, \dots, |\text{Path}_{od}|\}$. In practical applications, instead of using every possible integer value within this range, it is common to select breakpoints based on powers of two, such as $b_k \in \{1, 2, 4, 8, \dots\}$. This logarithmic spacing of breakpoints significantly reduces the number of linear segments and, consequently, the computational complexity of the model, while maintaining a high level of approximation accuracy for the reciprocal function.

In addition, the following decision variables are introduced.

- $y_{od} \geq 0$ —reciprocal of the number of active stations, that is, $y_{od} = 1/n_{od}$.

- $\theta_{od,k} \geq 0$ —auxiliary interpolation weights used for linearization. $\theta_{od,k}$ satisfy the special ordered set of type 2 (SOS2) property—meaning that at most two adjacent $\theta_{od,k}$ can take nonzero values [28].
- $s_{od,k} \in \{0, 1\}$ —binary interval-selection variables in the explicit SOS2 formulation.

The nonlinear flow-sharing formulation is given by:

$$n_{od} = \sum_{c \in \text{Path}_{od}} u_c, \quad \forall (o, d) \in O, \quad (13)$$

$$y_{od} = \frac{1}{n_{od}}, \quad \forall (o, d) \in O, \quad (14)$$

$$\lambda_{c,od} \leq \lambda_{od} y_{od}, \quad \forall c \in \text{Path}_{od}, \forall (o, d) \in O, \quad (15)$$

$$\lambda_{c,od} \leq \lambda_{od} u_c, \quad \forall c \in \text{Path}_{od}, \forall (o, d) \in O, \quad (16)$$

$$n_{od} \in \mathbb{Z}_+, \quad \forall (o, d) \in O, \quad (17)$$

$$y_{od} \geq 0 \quad \forall (o, d) \in O. \quad (18)$$

Equation (13) defines n_{od} as the number of active stations along O/D path (o, d) by summing the activation variables u_c . Equation (14) introduces y_{od} as the reciprocal of n_{od} , determining how demand is shared among the active stations. Note that, since each path must contain at least one active station (constraint (5)), division by zero cannot occur. Constraints (15) and (16) limit the assigned flow to feasible values: (15) ensures that each station can receive at most a fraction y_{od} of the total O/D demand, while (16)

prevents inactive stations from being allocated demand. A visual representation of a problem instance and corresponding solution can be seen in Figure 1.

The nonlinear reciprocal term $1/n_{od}$ in (14) is approximated using a piecewise linear function defined over the breakpoints b_k . To enable interpolation between consecutive breakpoints, the model introduces auxiliary weights $\theta_{od,k}$ that satisfy the SOS2 property—meaning that at most two adjacent $\theta_{od,k}$ can take nonzero values. This ensures smooth and accurate linear approximation of the nonlinear relationship.

Let K_{od} denote the ordered set of indices corresponding to the breakpoint values b_k used for the piecewise linear approximation of $1/n_{od}$, where each $b_k \in \{1, 2, \dots, |\text{Path}_{od}|\}$ (or a subset thereof, as discussed earlier). The corresponding linearized formulation replaces (14) with:

$$\sum_{k \in K_{od}} \theta_{od,k} = 1, \quad \forall (o, d) \in O, \quad (19)$$

$$n_{od} = \sum_{k \in K_{od}} b_k \theta_{od,k}, \quad \forall (o, d) \in O, \quad (20)$$

$$y_{od} = \sum_{k \in K_{od}} \frac{1}{b_k} \theta_{od,k}, \quad \forall (o, d) \in O. \quad (21)$$

Constraint (19) ensures that the $\theta_{od,k}$ variables form a convex combination. Equation (20) interpolates the value of n_{od} based on active breakpoints, while (21) defines y_{od} as the corresponding linear approximation of $1/n_{od}$. The SOS2 condition guarantees that interpolation occurs only between two consecutive b_k values,

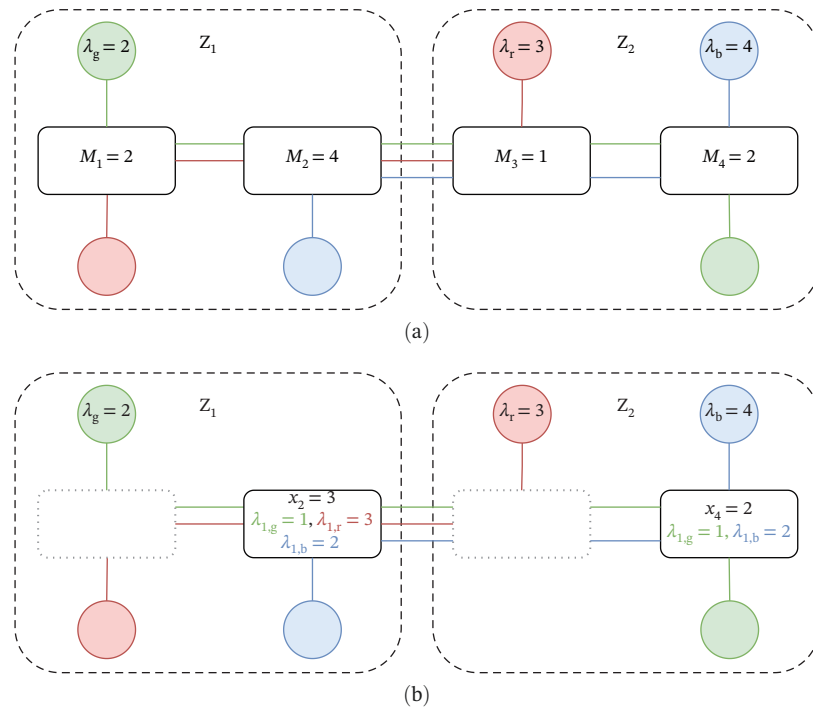


FIGURE 1 | Illustration of a model instance and its solution. Same-colored circles denote O/D pairs with hourly demand λ_{od} . Rectangles represent candidate charging stations, in the instance the label provides the maximum number of chargers (M_c) allowed at that station. The service rate is $\mu = 2$ and the QoS threshold is $\tau = 1$. Dashed rectangles indicate zones. Color-matched paths connect O/D pairs through the charging stations on their routes. In the solution, active stations ($u_c = 1$) have solid black borders, while inactive stations ($u_c = 0$) have dashed gray borders. For each station, the installed chargers (x_c) and the served O/D demand ($\lambda_{c,od}$) are shown. The total demand at active stations is $\Lambda_2 = 6$ and $\Lambda_4 = 3$, with corresponding service capacities ($\tau x_c \mu$) of 6 and 4, respectively. (a) Problem instance. (b) Solution.

producing a smooth linear approximation. In practice, most MILP solvers provide built-in SOS2 functionality, so these constraints are usually handled internally rather than explicitly implemented.

For the sake of completeness, the SOS2 property is provided explicitly as follows:

$$\sum_{k=1}^{|K_{od}|-1} s_{od,k} = 1 \quad \forall (o, d) \in O, \quad (22)$$

$$\sum_{k=1}^{|K_{od}|} \theta_{od,k} = 1 \quad \forall (o, d) \in O, \quad (23)$$

$$\theta_{od,1} \leq s_{od,1} \quad \forall (o, d) \in O, \quad (24)$$

$$\theta_{od,k} \leq s_{od,k-1} + s_{od,k} \quad \forall (o, d) \in O, k = 2, \dots, |K_{od}| - 1, \quad (25)$$

$$\theta_{od,|K_{od}|} \leq s_{od,|K_{od}|-1} \quad \forall (o, d) \in O, \quad (26)$$

$$s_{od,k} \in \{0, 1\}, \quad \forall (o, d) \in O k = 1, \dots, |K_{od}| - 1, \quad (27)$$

$$\theta_{od,k} \geq 0, \quad \forall (o, d) \in O k = 1, \dots, |K_{od}|. \quad (28)$$

Here, the binary variables $s_{od,k}$ determine which segment of the piecewise linear function is active for each O/D pair. Constraint (22) ensures that exactly one interval is selected, while (23) maintains the convex combination of $\theta_{od,k}$. Constraints (24)–(26) restrict positive $\theta_{od,k}$ values to the active segment, and (27),(28) define the variable domains. Together, these reproduce the SOS2 behavior, ensuring that only two consecutive $\theta_{od,k}$ values can be nonzero for any (o, d) pair.

Note that the Constraints (13)–(15) describe how demand is split proportionally among stations along a route. This proportional rule is a simple and tractable starting point for system-wide planning. However, the linearization method we use is not tied to this specific rule. The parameter y_{od} can be redefined to represent any station-specific allocation factor—for example, a probability from a driver choice model. This means the model could later include more realistic driver behavior, without losing linearity, as long as the new y_{od} can be expressed or approximated using the decision variables.

3 | Instance Generation

This section presents the method for converting real-world transport systems into problem instances. The focus is on single highways and a single direction, as EV charging infrastructure can largely be analyzed independently and drivers rarely use stations in the opposite direction. This approach allows precise modeling of traffic, charging demand, and station use while avoiding the complexity of multi-highway interactions. It simplifies data collection, reduces computational effort, and still captures the essential dynamics of highway EV charging behavior, providing a realistic yet tractable framework for evaluating station placement and performance. In the following text, the details of generating instance are provided. Specifically, the used data sources, the method for estimating EV charging demand on O/D pairs, and the procedure for converting this information into MILP instance parameters are detailed in the following text.

3.1 | Data Sources

The highway data for this study was obtained from Natural Earth Roads [29], providing vector road data at a 1:1,000,000 scale (up to 1:250,000 for some features). In North America, “basic” roads come from the CEC North America Environmental Atlas, while “supplementary” data includes attributes such as route number, road class, type, divided status, and state/province. Although higher-resolution maps like OpenStreetMap (OSM) exist, they are computationally expensive to process for large-scale instance generation. Natural Earth Roads offers a practical balance between spatial detail and efficiency, suitable for modeling EV charging infrastructure along highways.

The population data for cities used in this study are obtained from the GeoNames database [30]. Only cities with more than 1000 inhabitants were considered. The dataset includes information such as city name, geographic coordinates (latitude and longitude), population, and administrative hierarchy. GeoNames is a widely used open-source geographical database that integrates data from multiple public sources and provides global coverage with millions of place names. For convenience and consistency, the data was downloaded in a tabular format from the Open-DataSoft platform [31].

The potential locations for EV charging stations in this study are based on the locations of existing gas stations. The data for these locations was obtained from Geofabrik’s OSM extracts [32]. Geofabrik provides regularly updated, open-access geographic data derived from the OSM project, organized by continent and country. For this study, point-of-interest (POI) data was downloaded for individual U.S. states, and potential sites were filtered using the criterion `custom_filter = {“amenity”: [“fuel”]}`.

3.2 | Selection of Highway Segments, Cities, and Potential Charging Stations

This section outlines the methodology used to select the relevant highway segment, nearby cities, and potential locations for EV charging stations. The highway geometry is extracted from the Natural Earth Roads dataset based on a bounding box of a state, as well as the prefix and route number identifying the highway. This extraction yields a polyline representing the geographical alignment of the selected highway segment.

Relevant cities are identified according to their spatial proximity to the highway. Specifically, a city is considered associated with the highway if its minimum distance to the highway path is less than $d_c = 10$ km. The distance is computed using the Haversine formula between the city’s coordinates and the closest point along the highway polyline. Potential charging station sites are determined using the same spatial filtering approach, just using a maximum distance of $d_s = 1$ km from the highway. This procedure ensures that both urban areas and possible charging infrastructure are consistently aligned with the chosen highway segment.

3.3 | Procedure for Generating O/D Pairs, Zones, and Traffic Flow Generation

As previously stated the focus of the computational experiments is on the analysis of charging infrastructure on a single highway

in a single direction. This restriction makes it possible to represent the location of each cities and charging station using a single value l , the distance along highway. The value is calculated for each city and charging station by first calculating the closest point on the highway polyline to the corresponding position based on the latitude and longitude. Each such point gets a value based on the distance along the highway, calculated using the highway path, to be more precise using the corresponding shape file where the starting 0 position corresponds to the first point of the highway in the corresponding shape file. In the following text the notation l_a will be used for the value of the distance along highway for a city or charging station a . During the selection of charging stations, an additional filtering step was applied. In some cases, multiple stations had identical or nearly identical l values; in such cases, only a single station was retained at that location. Similarly, cities with negligible differences in the l value were merged into a single entity, whose population was set equal to the sum of the populations of the merged cities.

Zones are defined by dividing the highway into consecutive segments of length δ . Each charging station $c \in C$ with location l_c satisfying $(z-1)\delta < l_c \leq z\delta$ is assigned to zone z . In the generation of instances the value of δ is set to 75 km.

The set of O/D pairs O has been created using the following procedure. Firstly, all cities i and j are considered for an O/D pair if $l_i < l_j$, or in other words if city i is before city j on the selected direction of the highway. A charging station c will be on O/D pair (i, j) , $c \in \text{Path}_{ij}$, if $l_i \leq l_c \leq l_j$. Next, all O/D pairs that do not contain any charging stations are removed from the set of O/D pairs O .

The traffic flow between an O/D pair is estimated using a gravity-based model, where flow increases with the populations of the connected cities and decreases with distance. Although more advanced variants of the gravity model exist [33], the basic formulation is sufficient for the scope of this study. The model is defined as

$$T_{od} = \frac{P_o P_d \nu_d}{D_{od}^\alpha}, \quad (29)$$

where P_o and P_d represent the populations of the origin and destination cities, respectively; ν_d is a destination attractiveness factor (e.g., number of points of interest); D_{od} denotes the distance between the cities (in kilometers); and α is the distance decay exponent that controls how rapidly flow decreases with distance. In the conducted experiments, the attractiveness factor is assumed to be constant, that is, $\nu_d = 1$ for all destinations.

To better approximate charging demand rather than general traffic volume, a correction factor is introduced to account for the likelihood of charging events based on trip length. Short trips rarely require charging, while longer ones may necessitate multiple stops. The expected number of charging events for an O/D pair is approximated as

$$E_{od} = \frac{D_{od}}{r_{EV} \cdot \eta}, \quad (30)$$

where r_{EV} denotes the average driving range of an EV (km per full charge) and η is the utilization factor representing the fraction of the range typically used before recharging (i.e., accounting

for driver comfort and safety margins). The final estimated charging flow between the origin and destination is then given by

$$C_{od} = T_{od} \cdot E_{od}. \quad (31)$$

This formulation thus integrates both spatial interaction effects and charging behavior, providing a simple yet interpretable estimate of EV charging demand along intercity routes.

The parameters used in the experiments were $\alpha = 1.2$, $r_{EV} = 300$ km, and $\eta = 0.75$. For simplicity, it is assumed that the destination attractiveness factor $\nu_d = 1$ for all cities.

The estimated charging flows C_{od} are further used to generate the actual number of charging events in the model. Since the objective is to evaluate charging infrastructure performance under different levels of EV adoption, a total hourly charging demand T_c is assumed. The raw charging flows are normalized so that their sum equals the target demand:

$$\lambda_{od} = T_c \cdot \frac{C_{od}}{\sum_{(o',d') \in O} C_{o'd'}}. \quad (32)$$

This normalization ensures that the total number of simulated charging events reflects a desired system-wide adoption level, while preserving the relative distribution of demand among O/D pairs. Finally, O/D pairs with fewer than 0.2% of the total number of charging request per hour are excluded from the analysis to maintain computational efficiency and focus on significant traffic flows. A visual illustration of generating O/D pairs can be seen in Figure 2.

The generated O/D set emphasizes dominant demand corridors to maintain tractability. While this approach may not capture every possible trip, it focuses the optimization on high-volume flows that determine the backbone of the charging network. Consequently, certain low-volume or niche trips may not be explicitly represented, which could affect local demand patterns in specific segments. The zoning requirement (Constraint (4)) further ensures continuous spatial coverage along the highway, mitigating the impact of any omitted low-volume pairs on overall network connectivity.

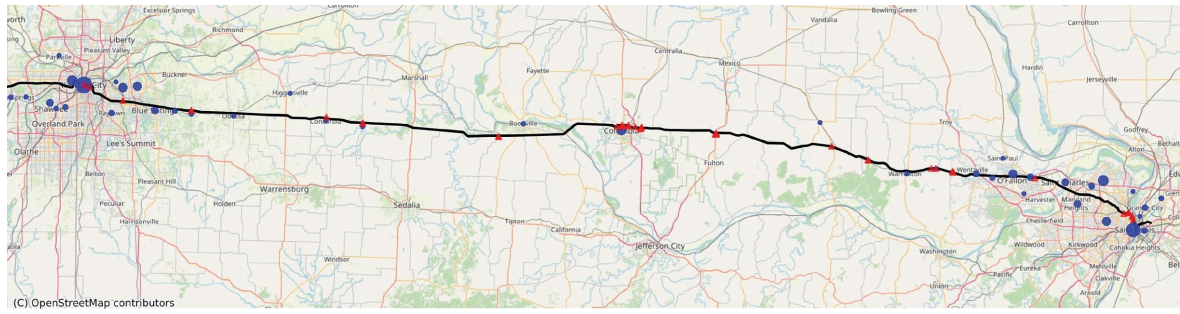
3.4 | Other Parameters

For simulation purposes, the charging time and service rate μ (number of vehicles charged per hour) are calculated assuming ideal constant power delivery. The charging fractions that is considered: is 70% of the battery capacity, representing uncertainty in the average SoC upon arrival. It is assumed that the vehicles have the same battery capacity $C_{bat} = 50$ kWh Charging times are computed as

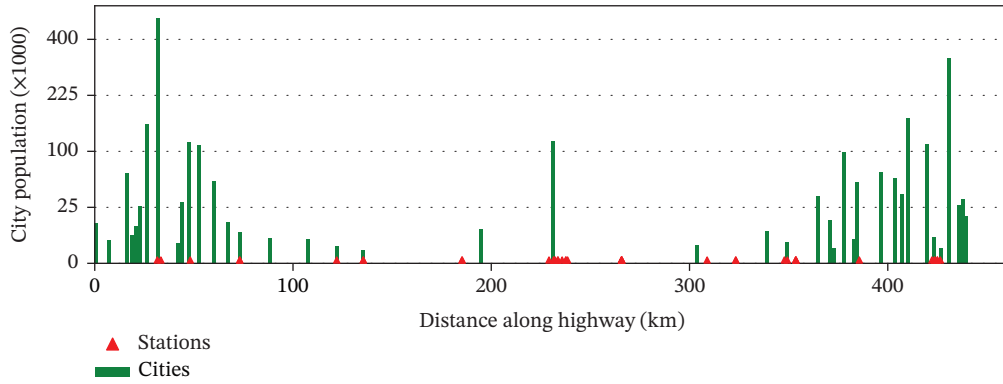
$$t = \frac{E_{delivered}}{P_{charger}},$$

where $E_{delivered}$ is the energy required ($0.7 \times C_{bat}$) and $P_{charger}$ is the rated power. The corresponding number of charges per hour is simply the reciprocal value, $\mu = 1/t$.

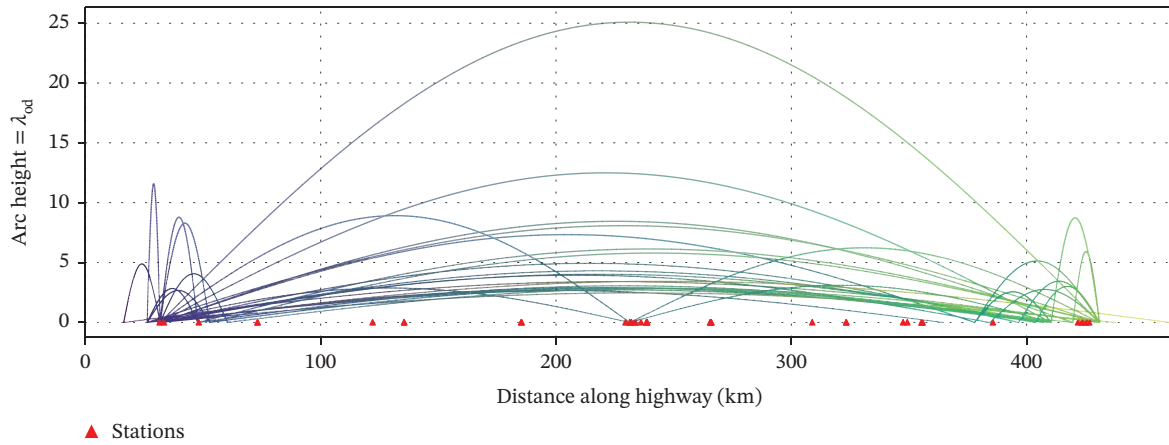
The parameter τ is a QoS coefficient limiting station utilization to prevent overloading, as defined in constraint (8). It ensures



(a)



(b)



(c)

FIGURE 2 | Generation of O/D pairs for Interstate I-70 in Missouri at $T_c = 300$. Blue circles indicate city locations scaled by population. Arcs connect selected O/D pairs; only the top 80% of pairs are shown for visual clarity. (a) Original map data. (b) City populations, locations, and potential charging station sites along the highway. (c) Generated O/D pairs.

stations operate below full capacity, maintaining service reliability. In this study, $\tau = 0.8$ was used, allowing operation up to 80% of maximum load.

The maximum number of chargers at station c , denoted M_c , was determined assuming a uniform station power limit of $P_{\text{station}} = 2$ MW. This value reflects typical constraints of medium-voltage grid connections. Accordingly, the maximum number of chargers was computed as

$$M_c = \left\lfloor \frac{P_{\text{station}}}{P_{\text{charger}}} \right\rfloor, \quad (33)$$

ensuring that the total installed charging capacity does not exceed the station's available power supply.

4 | Case Study Design and Analysis

To evaluate the applicability and performance of the proposed model, a set of representative highway corridors in the United States is analyzed. The selected highways differ in geographic, demographic, and structural characteristics, allowing the assessment of the model under diverse spatial and demand conditions.

- Interstate I-70 in Missouri: links two large urban centers, Kansas City and St. Louis, with a medium-sized city (Columbia) situated approximately halfway along the route, representing a more balanced O/D structure. The total population near the selected route is around 2.3 million. The analyzed highway section spans ~450 km and includes 25 potential charging station locations.

- Interstate I-95 in Florida: a long coastal highway serving numerous medium-sized urban areas and dense tourist regions, allowing testing of the model in settings characterized by distributed demand and seasonal variability. The total population near the selected route is around 6 million. The analyzed highway section spans ~600 km and includes 38 potential charging station locations.

The objective of the conducted case study is to analyze the impact of using chargers with different power ratings on both the total system cost and the expected time in the system (including charging and waiting times). The analysis considers chargers rated at 50, 150, and 350 kW, evaluated under varying EV adoption. The level of adoption is represented by the total number of charging requests per hour in the system, denoted as T_c . This approach enables the examination of how the structure and distribution of the charging infrastructure along the highway evolve with increasing charging demand.

The total hourly charging demand T_c was set to 100, 200, and 300 for the I-10 highway, which connects cities with a combined population of ~2.3 million. For comparison, on a 450 km segment of I-70 in Missouri with an approximate annual average daily traffic (AADT) of 50,000 [34] and an average trip length of 90 km, roughly 250,000 vehicles travel daily. Assuming 10% EV adoption and that 10% of EVs require charging, this corresponds to about 2500 charging sessions per day, or ~100 per h. For the I95 corridor, with a surrounding population of about 6 million, values of 250, 500, and 750 were used for T_c .

The model presented is outlined in Section 2, based on the formulations in (1)–(13) and (15)–(28) was used in the case study. The implementation was carried out in C#.NET using ILOG CPLEX with Concert Technology. Computational experiments

TABLE 1 | Representative cost ranges for EV charger installations (hardware + typical installation), adapted from [35].

Charger type	Power (kW)	Cost range (USD)
Medium DC fast	50	20,000–35,800
High DC fast	150	75,600–100,000
High-power DC	350	128,000–150,000

were performed on a Windows 10 workstation equipped with an Intel(R) Xeon(R) Gold 6244 CPU @ 3.60 GHz and 128 GB RAM. Each scenario was solved within one to 5 min.

4.1 | Cost and QoS

The first aspect of the EV charging infrastructure analyzed using the proposed model is the total installation cost. The analysis focuses on chargers rated at 50, 150, and 350 kW. Installation costs, including hardware, site preparation, electrical infrastructure, and typical setup expenses, are based on aggregated real-world data from [35]. Their study reports total project cost ranges per charger, derived from sources such as the Rocky Mountain Institute and the California EV Infrastructure Project, and accounts for variability due to regional factors, permitting, and project scale. These ranges, summarized in Table 1, ensure that the cost-minimization results reflect realistic deployment scenarios across different site conditions.

Another key metric is the expected time an EV spends at a charging station. It is estimated using an M/M/c queueing model, where c is the number of chargers at station and λ the arrival rate at the station [36]. The service rate assumes a 50 kWh battery with 70% average charging need (μ), capturing both waiting and charging times.

To better understand system behavior, several infrastructure characteristics are also analyzed: total number of active stations, total installed chargers, and average expected time in the system. At the station level, the variation in the number of chargers and the minimum and maximum expected service times are examined.

Results for the total infrastructure cost are presented in Table 2, while operational and structural indicators are summarized in Table 3. The results indicate that the use of 350 kW chargers generally provides a clear economic advantage over lower-power alternatives. For almost all tested values of T_c and across both analyzed highway segments, the 350 kW option resulted in the lowest total installation cost. The only exception occurred for the lowest EV adoption scenario on the I-70 corridor, where its cost slightly exceeded that of the 50 kW configuration. This can be attributed to the limited utilization of high-power chargers under low-demand conditions, where installation costs dominate over throughput benefits.

TABLE 2 | Total cost of EV charging infrastructure for different charging powers of chargers for different number of hourly charges.

Total charges (T_c)	50 kW	150 kW	350 kW
Interstate I-70 in Missouri			
100	1500–2685	2041–2700	1536–1800
200	3000–5370	3856–5100	2816–3300
300	4500–8055	5670–7500	4224–4950
Interstate I-95 in Florida			
250	3760–6730	4763–6300	3584–4200
500	7500–13,425	9450–12,500	6912–8100
750	11,260–20,155	14,213–18,800	10,496–12,300

Note: The costs are give in 1000 USD values.

TABLE 3 | Summary of charging station statistics for all experiments on Interstates I-70 (Missouri) and I-95 (Florida).

T_c	Power (kW)	Total			Per station			
		Stations	Chargers	Avg. Exp. time (h)	No. of chargers		Exp. time (h)	
					Min	Max	Min	Max
Interstate I-70 in Missouri								
100	50	12	75	0.88	4	10	0.72	1.05
	150	12	27	0.43	2	3	0.27	0.56
	350	10	12	0.35	1	2	0.12	0.43
200	50	10	150	0.67	12	19	0.64	0.69
	150	9	51	0.29	4	7	0.25	0.35
	350	10	22	0.21	2	3	0.14	0.24
300	50	9	225	0.63	19	33	0.61	0.64
	150	12	75	0.29	5	10	0.24	0.31
	350	9	33	0.15	3	5	0.12	0.18
Interstate I-95 in Florida								
250	50	13	188	0.68	8	21	0.63	0.77
	150	14	63	0.35	2	7	0.26	0.56
	350	12	28	0.21	1	3	0.12	0.43
500	50	16	375	0.64	15	40	0.61	0.66
	150	14	125	0.25	6	13	0.23	0.29
	350	16	54	0.17	2	5	0.13	0.24
750	50	25	563	0.65	5	40	0.61	0.93
	150	25	188	0.28	4	13	0.23	0.35
	350	28	82	0.19	2	5	0.12	0.24

Note: Results are shown for different total charging demand levels T_c and charger power ratings. Columns report the total number of stations and chargers, average expected charging and queueing time, and per-station ranges for the number of chargers and expected charging and queueing time.

Another important observation from Table 3 is the near-linear relationship between the total infrastructure cost and the overall charging demand T_c . As T_c increases, costs grow proportionally, with only minor reductions in cost per charging event at higher demand levels due to improved utilization of installed capacity. This trend is also reflected in the total number of chargers, which scales almost linearly with T_c .

Furthermore, the total installed charging power (computed as the product of the number of chargers and their rated power) remains relatively consistent across different charger types for the same highway and T_c value. The only notable deviation from this pattern is again observed for the I-70 highway under low adoption levels, primarily due to additional capacity requirements at certain stations needed to ensure adequate coverage across all O/D pairs and service zones.

From this analysis, it can be concluded that the cost efficiency of different charger power levels is largely determined by the average cost per kilowatt of installed charging capacity. This relationship is evident in Table 2, where, for each combination of T_c and highway segment, the total infrastructure cost is approximately proportional to the cost per kilowatt associated with the respective charger type.

The advantages of 350 kW chargers become even more evident when examining the expected time at charging stations. Their

use reduces the average time in the system by ~70% compared to 50 kW chargers and by around 30% relative to 150 kW chargers. The corresponding expected times are ~0.67, 0.30, and 0.20 h for the 50, 150, and 350 kW charger types, respectively. Notably, for a relatively modest increase in total infrastructure cost, upgrading from 50 to 150 kW chargers can nearly halve the expected time at stations.

When considering the variation in expected times across stations, the 50 kW chargers exhibit relatively uniform performance, with differences between the best- and worst-performing stations typically below 20%. In contrast, for 350 kW chargers, the variation can be substantial—for example, expected times may range from 0.12 to 0.42 h in certain cases. This behavior reflects the limited number of high-power chargers per station, which can lead to pronounced waiting time spikes under demand surges. Conversely, lower-power stations, having more chargers, are less sensitive to fluctuations in demand, as charging time dominates the total time in the system.

4.2 | Charging Station Distribution

The final part of the analysis examines the spatial distribution and placement of the selected charging stations in relation to the increased EV adoption. The results reveal substantial differences in the optimized infrastructure configurations between the I-70

and I-95 highway segments. Two main factors explain these differences. First, the I-95 corridor has roughly three times the population of I-70, despite being only about 30% longer. Second, the population along I-95 is more evenly distributed across the entire corridor, whereas for I-70 it is concentrated around the two terminal cities, with only a single medium-sized city near the midpoint. The corresponding spatial layouts of cities, population densities, and selected charging station locations with their installed capacities for different levels of adoption are illustrated in Figures 3 and 4.

The behavior of charging infrastructure differs notably between highways and EV adoption levels. For the I-70 highway, the initial set of charging station locations is determined for the lowest EV adoption level ($T_c = 100$) and remains largely stable

as adoption increases to $T_c = 200$ and $T_c = 300$. The main change is an increase in the number of chargers at existing stations. Interestingly, for some charger power levels, the number of stations slightly decreases with higher adoption, likely due to population distribution: even at low adoption, many stations must be active to satisfy zone and origin/destination constraints.

In contrast, on I-95, the number of charging stations grows consistently with increasing adoption and is more uniformly distributed along the highway. Many stations reach their maximum charger capacity, driving expansion. Stations present at low adoption levels generally persist at higher levels.

For both highways, a similar set of locations is largely reused across scenarios, suggesting that upgrades in charger power at

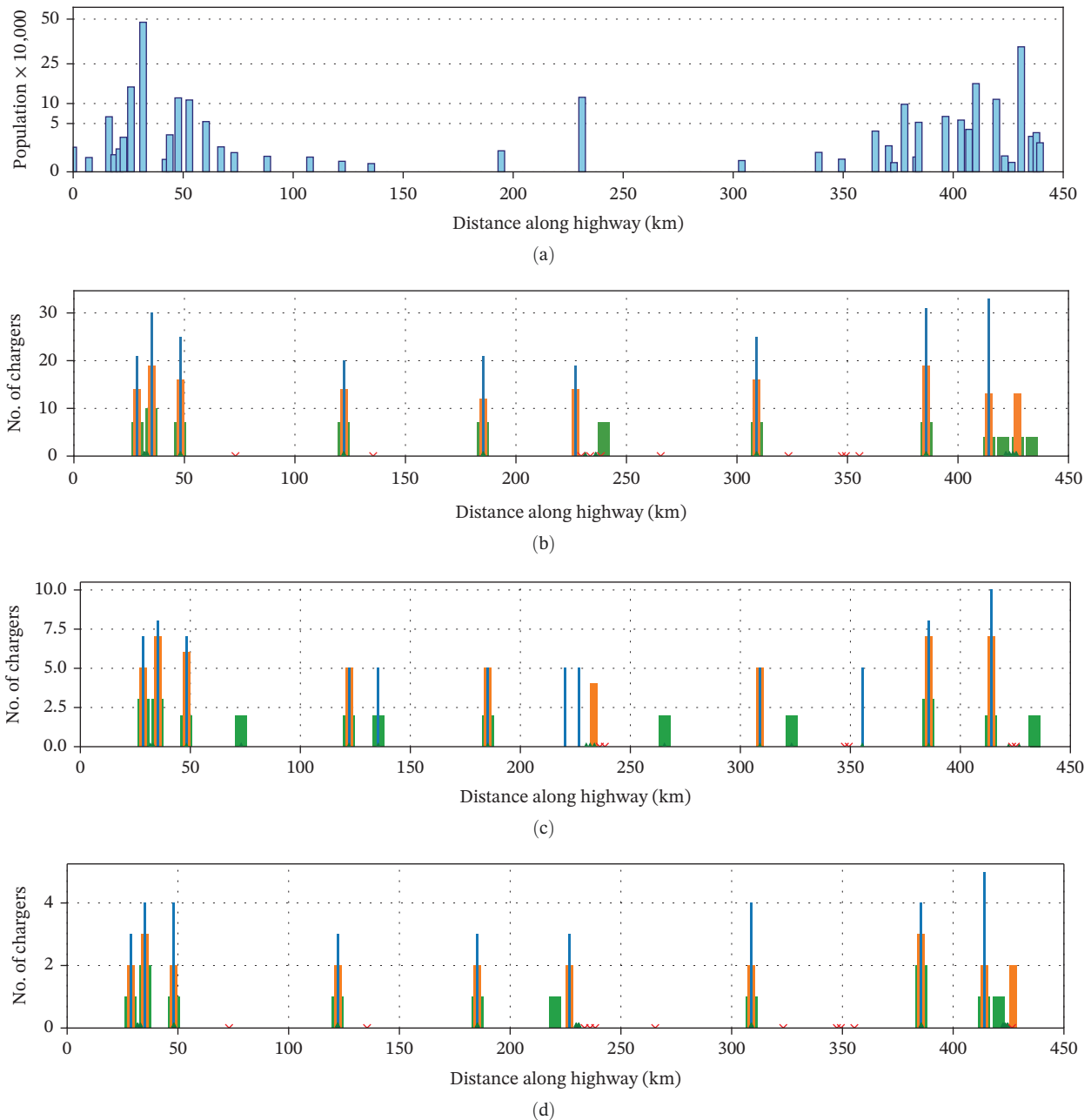


FIGURE 3 | Spatial distribution of cities and charging stations along Interstate I-70 in Missouri. The first subfigure (a) shows city locations, with bar heights proportional to city populations. The remaining subfigures (b–d) depict charging station locations and installed capacities for charger power levels of 50, 150, and 350 kW. Green, orange, and blue bars indicate the number of chargers for $T_c = 100$, $T_c = 200$, and $T_c = 300$, respectively. Overlapping colors denote the same station across multiple demand scenarios. (a) City populations. (b) 50 kW. (c) 150 kW. (d) 350 kW.

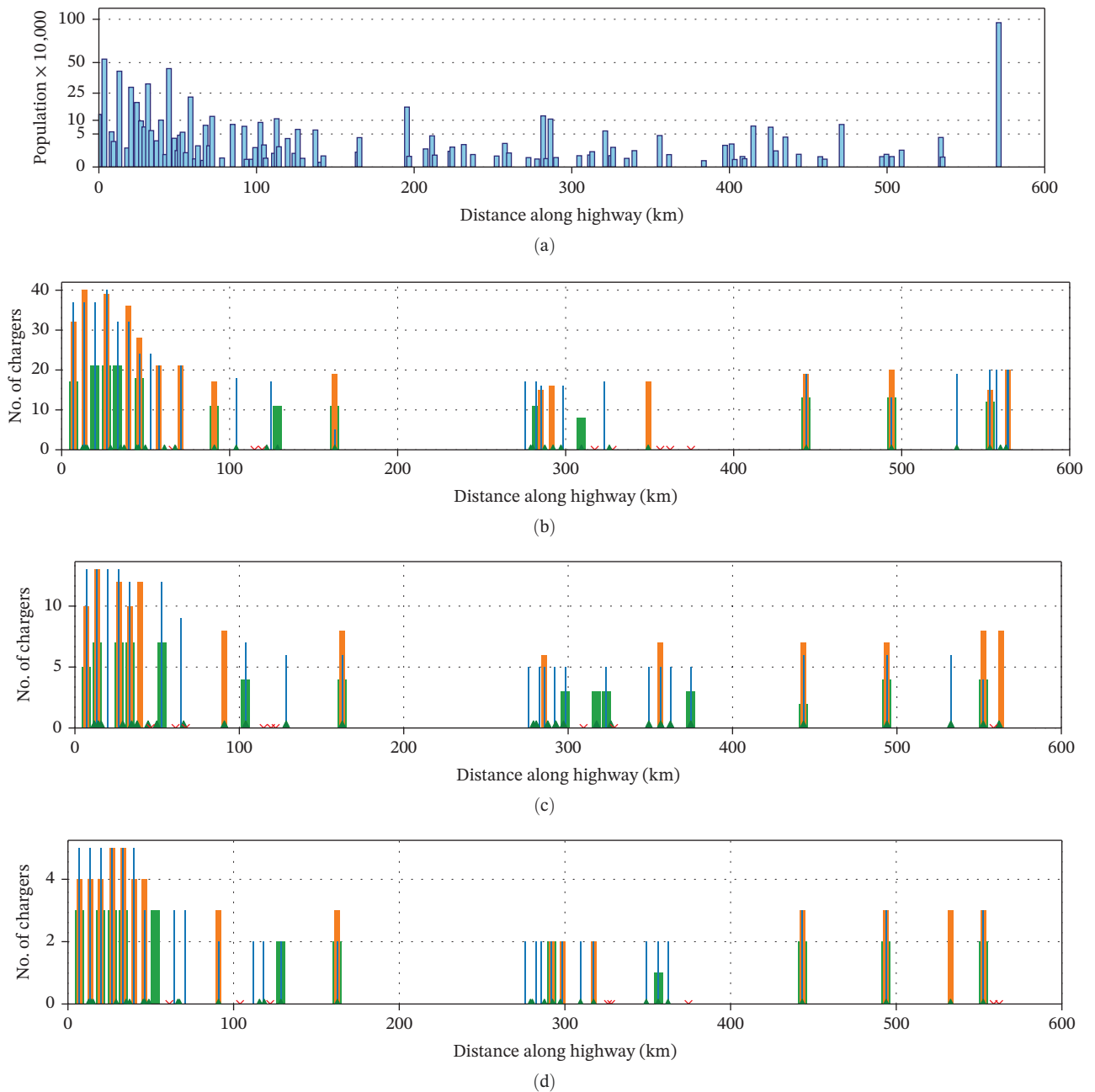


FIGURE 4 | Spatial distribution of cities and charging stations along Interstate I-95 in Florida. The first subfigure (a) shows city locations, with bar heights proportional to city populations. The remaining subfigures (b–d) depict charging station locations and installed capacities for charger power levels of 50, 150, and 350 kW. Green, orange, and blue bars indicate the number of chargers for $T_c = 250$, $T_c = 500$, and $T_c = 750$, respectively. Overlapping colors denote the same station across multiple demand scenarios. (a) City populations. (b) 50 kW. (c) 150 kW. (d) 350 kW.

existing stations could be implemented while maintaining a near-optimal spatial distribution of infrastructure.

4.3 | Robustness and Value Considerations

The multi-scenario analysis conducted in this case study serves as a practical robustness evaluation of the proposed model. The variation in total hourly demand, T_c , implicitly captures the combined influence of underlying behavioral and technological parameters. Specifically, EV range (r_{EV}) and battery utilization factor (η) determine the expected number of charging events per trip (Equations (30)–(32)); therefore, exploring different T_c values

assesses how infrastructure strategies adapt to changes in vehicle technology and driver habits. Concurrently, evaluating different charger power levels (50, 150, 350 kW) directly modifies the service rate μ , which interacts with the QoS coefficient τ in the capacity constraint (8). This setup allows the model to explore the fundamental trade-off between service capacity and capital expenditure under a wide range of planning assumptions.

The results from the varied scenarios allow us to directly observe how changes in the underlying parameters manifest in infrastructure outcomes. On the demand side, an increase in EV range (r_{EV}) or a higher battery utilization factor (η) reduces the number of required charging events per trip. In our model, this is

equivalent to a lower total demand T_c . Our results (Table 3) show that for a given charger power, lower T_c leads to fewer total chargers and a reduction in the number of active stations, particularly in corridors like I-95 where demand is more spatially distributed. Turning to service parameters, using a higher-power charger directly increases the service rate μ , which—for a fixed QoS level τ —allows each charger to serve more vehicles per hour. This effect is evident in the results (Tables 2 and 3): despite their higher unit cost, 350 kW chargers often yield a lower total system cost and significantly reduce expected user time because fewer total units are needed to meet the same demand T_c . Finally, the QoS parameter τ and service rate μ appear as a product in the capacity constraint (8), meaning that varying τ is proportionally equivalent to varying μ . Consequently, comparing different charger powers (which directly change μ) inherently tests the sensitivity of the solution to service-level requirements.

5 | Conclusion

This paper presented a MILP model for the strategic planning of EV charging infrastructure along highway corridors. The model determines the optimal locations and capacities of charging stations to minimize total investment cost while ensuring adequate coverage for all O/D pairs and maintaining a predefined QoS. A key contribution of the proposed formulation is the explicit modeling of how charging demand from each O/D pair is distributed among the multiple stations along its path. The inherent nonlinearity of this flow-sharing mechanism was effectively addressed using a piecewise linear approximation, resulting in a tractable model that can be solved for real-world-sized instances using standard MILP solvers.

The case study, conducted on two distinct U.S. highway corridors (I-70 in Missouri and I-95 in Florida), demonstrated the model's practical applicability and provided valuable insights. The analysis of different charger power ratings (50, 150, and 350 kW) under varying levels of EV adoption revealed a clear trade-off between infrastructure cost and service quality. The results indicate that high-power 350 kW chargers generally offer the most cost-effective solution, as their superior throughput allows for a lower total number of chargers to meet a given demand, despite their higher unit cost. Furthermore, the use of 350 kW chargers significantly reduces the expected time vehicles spend at stations—by ~70% compared to 50 kW chargers and 30% compared to 150 kW chargers—greatly enhancing user convenience.

The spatial analysis of the optimized infrastructure showed that the structure of the highway network and the distribution of population significantly influence the resulting station layouts. For the corridor with demand concentrated at its endpoints (I-70), the set of active stations remained relatively stable as adoption increased, with capacity expansion occurring primarily at existing locations. In contrast, for the corridor with more uniformly distributed demand (I-95), the number of stations grew more consistently with adoption. In both cases, a core set of optimal locations was identified, suggesting that infrastructure planning can be staged, with initial stations forming a backbone for future capacity upgrades.

For future research, several extensions of the model appear promising. Incorporating more sophisticated user choice models,

such as probabilistic station selection based on waiting times or pricing, could enhance behavioral realism. The model could also be extended to consider the integration of charging infrastructure with the power grid, including constraints on power availability and the potential for using on-site energy storage. Finally, exploring dynamic and multi-period investment strategies that account for the gradual evolution of EV adoption and technology costs would be a valuable direction for long-term infrastructure planning.

Funding

No funding was received for this manuscript.

Conflicts of Interest

The authors declare no conflicts of interest.

Data Availability Statement

The data that support the findings of this study are available from the corresponding author upon reasonable request.

References

1. B. Chen, H. Guo, F. Zhou, et al., "Electric Vehicle Users' Charging Patterns and Selection Considerations at Public Charging Stations," *Transportation Research Part D: Transport and Environment* 149 (2025): 105081.
2. M. Katontoka, F. Orsi, M. Bakker, and B. Hocks, "Toward Sustainable Transportation: A Systematic Review of Ev Charging Station Locations," *International Journal of Sustainable Transportation* 19, no. 10 (2025): 881–893.
3. International Energy Agency, "Global EV Outlook," (2025).
4. D. Clar-Garcia, M. Fabra-Rodriguez, H. Campello-Vicente, and E. Velasco-Sanchez, "Optimal DC Fast-Charging Strategies for Battery Electric Vehicles During Long-Distance Trips," *Batteries* 11, no. 11 (2025): 394.
5. I. S. Bayram, M. Devetsikiotis, and R. Jovanovic, "Optimal Design of Electric Vehicle Charging Stations for Commercial Premises," *International Journal of Energy Research* 46, no. 8 (2022): 10040–10051.
6. P. Brown, M. Contestabile, and R. Jovanovic, "A Mixed Integer Program for Optimizing the Expansion of Electrical Vehicle Charging Infrastructure," in *Modelling and Development of Intelligent Systems, 2021*, eds. D. Simian and L. F. Stoica, (Springer International Publishing): 302–314.
7. X. Li and A. Jenn, "An Integrated Optimization Platform for Spatial-Temporal Modeling of Electric Vehicle Charging Infrastructure," *Transportation Research Part D: Transport and Environment* 104 (2022): 103177.
8. H. M. Abdullah, A. Gastli, L. Ben-Brahim, and S. O. Mohammed, "Planning and Optimizing Electric-Vehicle Charging Infrastructure Through System Dynamics," *IEEE Access* 10 (2022): 17495–17514.
9. A. Awasthi, K. Venkitesamy, S. Padmanaban, R. Selvamuthukumar, F. Blaabjerg, and A. K. Singh, "Optimal Planning of Electric Vehicle Charging Station at the Distribution System Using Hybrid Optimization Algorithm," *Energy* 133 (2017): 70–78.
10. M. Choi, Y. Van Fan, D. Lee, S. Kim, and S. Lee, "Location and Capacity Optimization of Ev Charging Stations Using Genetic Algorithms and Fuzzy Analytic Hierarchy Process," *Clean Technologies and Environmental Policy* 27, no. 4 (2025): 1785–1798.

11. G. Zhou, Z. Zhu, and S. Luo, "Location Optimization of Electric Vehicle Charging Stations: Based on Cost Model and Genetic Algorithm," *Energy* 247 (2022): 123437.
12. P. Skaloumpakas, E. Spiliotis, E. Sarmas, et al., "A Multi-Criteria Approach for Optimizing the Placement of Electric Vehicle Charging Stations in Highways," *Energies* 15, no. 24 (2022): 9445.
13. Y. Wu, Y. Lu, Z. Zhu, and J. Holguín-Veras, "Optimizing Electric Vehicle Charging Infrastructure on Highways: A Multi-Agent-Based Planning Approach," *Sustainability* 15, no. 18 (2023): 13634.
14. A. Saldarini, S. M. Miraftebadeh, M. Brenna, and M. Longo, "Strategic Approach for Electric Vehicle Charging Infrastructure for Efficient Mobility Along Highways: A Real Case Study in Spain," *Vehicles* 5, no. 3 (2023): 761–779.
15. S. Micari, A. Polimeni, G. Napoli, L. Andaloro, and V. Antonucci, "Electric Vehicle Charging Infrastructure Planning in a Road Network," *Renewable and Sustainable Energy Reviews* 80 (2017): 98–108.
16. Y. Zhang, Z. Yin, H. Xiao, and F. Luo, "Coordinated Planning of Ev Charging Stations and Mobile Energy Storage Vehicles in Highways With Traffic Flow Modeling," *IEEE Transactions on Intelligent Transportation Systems* 25, no. 12 (2024): 21572–21584.
17. D. Xiao, S. An, H. Cai, J. Wang, and H. Cai, "An Optimization Model for Electric Vehicle Charging Infrastructure Planning Considering Queuing Behavior With Finite Queue Length," *Journal of Energy Storage* 29 (2020): 101317.
18. D. Hu, J. Zhang, and Q. Zhang, "Optimization Design of Electric Vehicle Charging Stations Based on the Forecasting Data With Service Balance Consideration," *Applied Soft Computing* 75 (2019): 215–226.
19. R. Jovanovic, S. Bayhan, and I. S. Bayram, "Capacity Optimization of EV Charging Networks: A Greedy Algorithmic Approach," in *2022 3rd International Conference on Smart Grid and Renewable Energy (SGRE)* (2022): 1–6
20. C. Kong, R. Jovanovic, I. S. Bayram, and M. Devetsikiotis, "A Hierarchical Optimization Model for a Network of Electric Vehicle Charging Stations," *Energies* 10, no. 5 (2017): 675.
21. A. J. Solic, D. Jakus, J. Vasilj, and D. Jolevski, "Electric Vehicle Charging Station Power Supply Optimization With v2x Capabilities Based on Mixed-Integer Linear Programming," *Sustainability* 15, no. 22 (2023): 16073.
22. M. Veisi, H. Naderian, and M. Karimi, "Optimal Charging Station Placement of Electric Vehicles in the Smart Distribution Network Based on the Mixed Integer Linear Programming," *International Journal of Electrical Power & Energy Systems* 168 (2025): 110675.
23. U. Chawal, J. Rosenberger, V. C. Chen, et al., "A Design and Analysis of Computer Experiments Based Mixed Integer Linear Programming Approach for Optimizing a System of Electric Vehicle Charging Stations," *Expert Systems With Applications* 245 (2024): 123064.
24. A. Mirheli and L. Hajibabai, "Hierarchical Optimization of Charging Infrastructure Design and Facility Utilization," *IEEE Transactions on Intelligent Transportation Systems* 23, no. 9 (2022): 15574–15587.
25. R. S. Gupta, A. Tyagi, and S. Anand, "Optimal Allocation of Electric Vehicles Charging Infrastructure, Policies and Future Trends," *Journal of Energy Storage* 43 (2021): 103291.
26. I. Rahman, P. M. Vasant, B. S. M. Singh, M. Abdullah-Al-Wadud, and N. Adnan, "Review of Recent Trends in Optimization Techniques for Plug-in Hybrid, and Electric Vehicle Charging Infrastructures," *Renewable and Sustainable Energy Reviews* 58 (2016): 1039–1047.
27. Y. Zhang, Y. Wang, F. Li, B. Wu, Y. Y. Chiang, and X. Zhang, "Efficient Deployment of Electric Vehicle Charging Infrastructure: Simultaneous Optimization of Charging Station Placement and Charging Pile Assignment," *IEEE Transactions on Intelligent Transportation Systems* 22, no. 10 (2021): 6654–6659.
28. E. M. L. Beale and J. A. Tomlin, "Special Facilities in a General Mathematical Programming System for Non-Convex Problems Using Ordered Sets of Variables," *Operational Research* 69, no. 4 (1970): 99.
29. N. Earth, "Natural Earth Roads," 2025, accessed: 2025-10-16 <https://www.naturalearthdata.com/downloads/10m-cultural-vectors/roads/>.
30. Unxos GmbH, "Geonames," 2025, accessed: 2025-10-16 <https://download.geonames.org/>.
31. opendatasoft.com, "Geonames All Cities with Population >1000," 2025, accessed: 2025-10-16 <https://public.opendatasoft.com/explore/assets/geonames-all-cities-with-a-population-1000/>.
32. G. GmbH, "Geofabrik Openstreetmap Data Extracts," 2025, Accessed: 2025-10-16 URL <https://download.geofabrik.de/>.
33. C. Thompson, K. Saxberg, J. Lega, D. Tong, and H. Brown, "A Cumulative Gravity Model for Inter-Urban Spatial Interaction at Different Scales," *Journal of Transport Geography* 79 (2019): 102461.
34. Missouri Department of Transportation, 2025, *Archived Traffic Volume Maps* <https://www.modot.org/archived-traffic-volume-maps> Accessed: 2025-10-16.
35. D. Bernal, A. A. Raheem, S. Inti, and H. Wang, "Assessment of Economic Viability of Direct Current Fast Charging Infrastructure Investments for Electric Vehicles in the United States," *Sustainability* 16, no. 15 (2024): 6701.
36. J. F. Shortle, J. M. Thompson, D. Gross, and C. M. Harris, *Fundamentals of Queueing Theory* (John Wiley & Sons, 2018).